Modelling and Identification of a Piezoelectrically Driven Fuel Injection Control Valve


```
@article{Mueller10,
  author = {M{\"u}ller, T. and Kugi, A. and Bachmaier, G. and Gerlich, M.},
  title = {Modelling and Identification of a Piezoelectrically Driven Fuel Injection Control Valve},
  journal = {Mathematical and Computer Modelling of Dynamical Systems},
  year = {2010},
  volume = {16},
  pages = {285--305},
  doi = {10.1080/13873954.2010.502027}
}
```

Mathematical and Computer Modelling of Dynamical Systems
Vol. 00, No. 00, May 2010, 1–20

Paper

Modelling and Identification of a Piezoelectrically Driven Fuel Injection Control Valve

T. Müller[a*], A. Kugi[a], G. Bachmaier,[b] and M. Gerlich,[b]

[a]*Automation and Control Institute (ACIN), Vienna University of Technology, 1040 Vienna, Austria*; [b]*Corporate Technology, Siemens AG, Munich, Germany*

(*January 2010*)

In this paper the modelling and identification of a piezoelectrically driven control valve of a common-rail diesel fuel injector in an experimental setup is presented. The piezoelectric actuator of the control valve exhibits a strong temperature dependence. Furthermore, an unknown mechanical parameter in the control valve mechanics, the idle stroke value, has to be determined. An optimization based method is used for temperature adaptation as well as for the identification of the unknown idle stroke value. Both, the suppression of the temperature dependence as well as the exact knowledge of the idle stroke value are essential for the opening width and opening point of time of the control valve and thus for the accuracy of the fuel injection. The identification task becomes even more challenging since only the electrical signals of the actuator, voltage and current, are measurable. The method is successfully validated in an experimental setup.

Keywords: fuel injection, piezoelectric stack actuator, hybrid system, identification, switching system, idle stroke detection

AMS Subject Classification: F1.1; F4.3 **(... for example; authors are encouraged to provide two to six 2000 Mathematics Subject Classification codes)**

1. Introduction

Direct fuel injection is state-of-the-art for modern diesel engines in passenger cars and is increasingly used in gasoline car engines. It allows to inject fuel almost independent of the working cycle of the engine. This additional degree of freedom is used to adapt the combustion process to changing working conditions in order to reduce fuel consumption, noise and emissions. Especially for diesel engines it is common to use multiple fuel injections with different injection durations and quantities in one engine cycle. For a further reduction of emissions and consumption the number of fuel injections as well as the accuracy in time and quantity has to be increased. An essential limitation for multiple injections with small fuel quantities is the dynamics of the control valve of the injector. The faster the control valve reacts to a fuel injection input signal the more individual injections with higher precision can be done. For this reason piezoelectrically driven control valves have been introduced as their dynamics are distinctively faster than those of the commonly used magnetic control valves [1].

In this paper, we investigate such a piezoelectrically driven control valve. It is a part of a common-rail diesel fuel injector and is integrated in an experimental

*Corresponding author. Email: mueller@acin.tuwien.ac.at

ISSN: 1387-3954 print/ISSN 1744-5051 online

DOI: 10.1080/1387395YYxxxxxxxx
http://www.informaworld.com

setup. For driving the control valve, a current controlled power amplifier, which basically corresponds to the amplifier used in series-production vehicles, is applied with all the inherent limitations to the input signal generation. The complete setup is presented in detail in Section 2.

The core of the piezoelectrically driven control valve is a piezoelectric stack actuator (PSA). PSAs consist of up to several hundred stacked layers of piezoelectric material, mostly lead zirconate-titanate (PZT) ceramics, that are connected to the power amplifier. PZT ceramics strongly depends on temperature and exhibits a nonlinear behaviour, mainly hysteresis, in large-signal operation. Therefore, one focus of the paper is on finding an appropriate model of the PSA that can be easily adapted to changes in the temperature. The challenge herein is that only the actuator voltage and current signals are available for the identification. In Section 3, existing stack actuator models are discussed and a model for the specific application is presented. Experimental results of the adaptation to different temperatures via voltage and current signals are shown. Furthermore, the adaptation is applied to several PSAs to investigate the robustness of the proposed method with respect to variations in the PSA series production. The use of only electrical signals for the identification requires – at least in parts – a high accuracy of the model, especially since the model is used for the additional identification of an unknown mechanical parameter, namely the so called idle stroke of the valve.

Between the PSA and the valve piston there is a small gap in the micrometer range. It helps to prevent constant opening of the control valve as the length of the gap varies, e.g. with fuel pressure when the valve plunger is pressed deeper into its seat or with aging. The width of the gap is essential for the opening width and the opening point of time of the control valve. If it is too small the valve opens too early. If it is too large the valve opens too late, not far enough or even not at all. Since the actuator elongates without opening the valve before getting into contact with the valve piston, we call this gap the idle stroke of the PSA. For opening the control valve with a desired stroke this value has to be known, especially since the maximum elongation of the used PSA in standard operation is $30\,\mu$m to $40\,\mu$m. Furthermore, the exact adjustment of the idle stroke value is quite cumbersome in the production of the fuel injection system. The idle stroke value cannot be measured in operation and even in the assembling of the fuel injection system only indirect measurements are possible. Therefore, the identification of the idle stroke value is the second focus of this paper. The identification is only performed on the basis of the electrical signals. The effect of changes in the idle stroke on the voltage signal turns out to be relatively small.

Due to this idle stroke the mathematical model of the control valve possesses a switching structure. The modelling of the contact between the PSA and the valve piston as well as the opening of the valve requires to switch between different continuous systems. The switching point is not known in advance but depends on the model state as well as on the idle stroke value and the opening force.

While in literature many publications on the modelling of PSAs and the compensation of their nonlinearities can be found, see, e.g., [2–6, 17], one finds only few results on the identification and modelling of piezoelectrically driven fuel injection systems. Wang [7] has proposed a highly parametrized PSA model that can be adapted to temperature changes via polynomial approximations of experimentally determined characteristic curves. This model is used by Raupach [8] to reconstruct an external force on the PSA in order to detect opening points in a fuel injection control valve. Mehlfeldt et al. [9] present a model of a fuel injection system and describe different PSA models. They do neither consider the change of the PSA behaviour with temperature nor do they identify the idle stroke value.

Post-print version of the article: T. Müller, A. Kugi, G. Bachmaier, and M. Gerlich, "Modelling and identification of a piezoelectrically driven fuel injection control valve", *Mathematical and Computer Modelling of Dynamical Systems*, vol. 16, pp. 285–305, 2010. DOI: 10.1080/13873954.2010.502027

2. Experimental Setup

The experimental setup of the piezoelectrically driven control valve is shown in Figure 1. The PZT stack is located in the center of the figure. For preloading, the PZT stack is clamped by a tube shaped spring between a top and a bottom plate. The top plate is welded to the PSA housing. Together with the electric connectors those are the basic parts of the PSA. For centering the PSA, the PSA housing is connected to two bushings via a clamping ring. The inner bushing, the fixing bushing, presses the PSA housing via the clamping ring into the adjustment bushing. The adjustment bushing allows to adjust the gap between the bottom plate of the actuator and the valve piston (idle stroke) by a fine pitch thread. The gap itself cannot be measured directly. However, for calibration purposes the gap between the adjustment bushing and the base body can be measured by a dial gauge with a resolution of one micrometer.

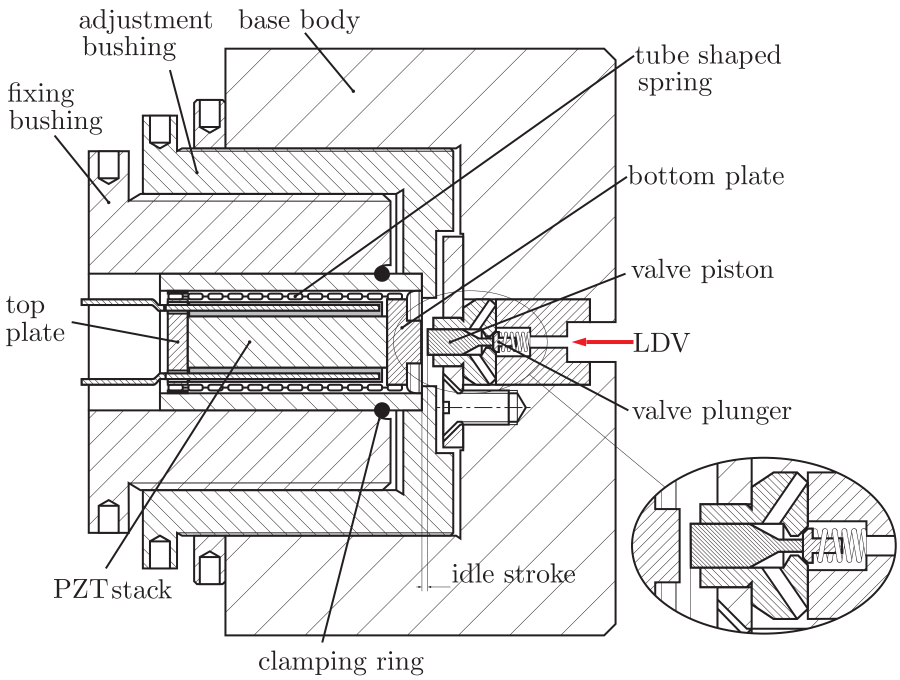

Figure 1. Experimental setup.

When the actuator is operated, the PZT stack elongates and moves the PSA bottom plate in the direction of the valve piston. The valve piston opens the valve by lifting the valve plunger out of its seat against the valve spring. The preloaded valve spring guarantees the closure of the valve. The PSA has to move against the valve spring and, under real operating conditions, also against the pressure force of the fuel that is present in the volume around the valve spring. For the experiment a Laser-Doppler vibrometer (LDV) is used for measuring the displacement of the valve plunger. By removing the control valve the LDV can also be used for measuring the displacement of the PSA bottom plate. The whole setup is mounted on the base body. The base body can be cooled or heated by a temperature control system in the temperature range normally used in automotive applications. An important issue in the experimental setup design is the high stiffness in the mounting of the PSA.

Post-print version of the article: T. Müller, A. Kugi, G. Bachmaier, and M. Gerlich, "Modelling and identification of a piezoelectrically driven fuel injection control valve", *Mathematical and Computer Modelling of Dynamical Systems*, vol. 16, pp. 285–305, 2010. DOI: 10.1080/13873954.2010.502027

For driving the actuator a current controlled two-quadrant chopper (buck-boost) power amplifier is used which corresponds to the amplifier used in series production of piezoelectric valves.

3. Modelling the PSA

3.1. *Linearized constitutive equations of piezoelectricity*

In general the linearized constitutive equations of piezoelectricity, see, e.g., [10–12], form the basis for piezoelectric actuator models. In their standard formulation no distinction between isothermal and adiabatic material constants is made, and slow changes in temperature and entropy compared to the actuator dynamics are assumed [10]. Then the state of the material is characterized by the mechanical variables stress σ_{ij} and strain ε_{kl}, $i, j, k, l = 1, 2, 3$, and the electric variables electric field E_m and electric displacement (or flux density) D_i, $m, i = 1, 2, 3$. The temperature T is assumed to be constant. Depending on the choice of the independent variables different formulations do exist. In this paper, we consider the constitutive equations [12]

$$\sigma_{ij} = c^{E,T}_{ijkl}\varepsilon_{kl} - e^{T}_{mij}E_m \quad \text{and} \tag{1}$$

$$D_n = e^{T}_{nkl}\varepsilon_{kl} + \epsilon^{\varepsilon,T}_{nm}E_m \tag{2}$$

with the elasticity coefficients $c^{E,T}_{ijkl}$ at constant electric field and temperature, the piezoelectric coefficients e^{T}_{mij} at constant temperature and the dielectric coefficients $\epsilon^{\varepsilon,T}_{nm}$ at constant strain and temperature.

These equations are used for modelling the PZT stack shown in Figure 2. The stack of length L and cross sectional area A consists of N PZT layers (in grey) separated by thin electrodes (thick black lines). The PZT layers are driven electrically in parallel by a power amplifier with voltage U and current I. At the two ends of the stack the force F is present.

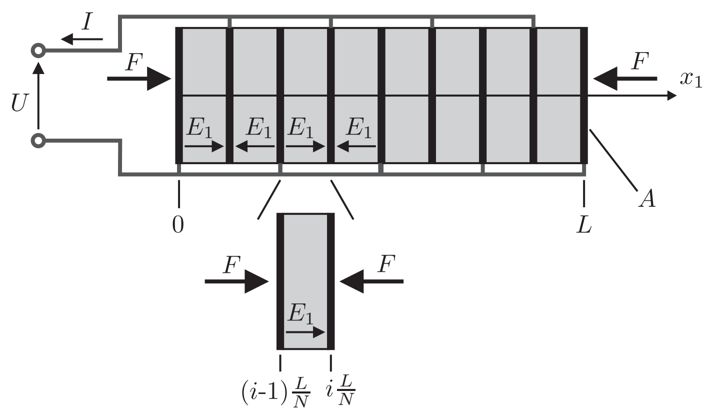

Figure 2. Model of a PZT stack with N layers.

For the electric field it is assumed that the components E_2 and E_3 are identically zero. Furthermore, only a uniaxial state of stress is considered with all components σ_{ij} equal to zero except for σ_{11}. In the geometric linearized scenario, the longitu-

Post-print version of the article: T. Müller, A. Kugi, G. Bachmaier, and M. Gerlich, “Modelling and identification of a piezoelectrically driven fuel injection control valve”, *Mathematical and Computer Modelling of Dynamical Systems*, vol. 16, pp. 285–305, 2010. DOI: 10.1080/13873954.2010.502027
The content of this post-print version is identical to the published paper but without the publisher’s final layout or copy editing.

dinal strain ε_{11} is related to the deflection of the stack $u(x_1)$

$$\varepsilon_{11} = \frac{\partial u(x_1)}{\partial x_1} \,. \tag{3}$$

Thus, by accounting for these assumptions in (1) and integrating over the stack volume V one obtains

$$\int\limits_V \sigma_{11} \mathrm{d}V = \int\limits_V \left(c_{1111}^{E,T} \varepsilon_{11} - e_{111}^{T} E_1 \right) \mathrm{d}V \tag{4}$$

$$\sum_{i=1}^{N} \int\limits_{(i-1)\frac{L}{N}}^{i\frac{L}{N}} \int\limits_A \sigma_{11} \mathrm{d}A \mathrm{d}x_1 = \sum_{i=1}^{N} \int\limits_{(i-1)\frac{L}{N}}^{i\frac{L}{N}} \int\limits_A \left(c_{1111}^{E,T} \frac{\partial u}{\partial x_1} - e_{111}^{T} E_1 \right) \mathrm{d}A \mathrm{d}x_1 \tag{5}$$

$$\underbrace{\sigma_{11} A}_{=F} L = A c_{1111}^{E,T} \underbrace{\sum_{i=1}^{N} \left(u(i\frac{L}{N}) - u((i-1)\,\frac{L}{N}) \right)}_{=(u(L)-u(0))} - A e_{111}^{T} N \underbrace{E_1 \frac{L}{N}}_{=U} \tag{6}$$

$$F = \underbrace{\frac{A c_{1111}^{E,T}}{L}}_{=:k} (u(L) - u(0)) - \underbrace{\frac{A N e_{111}^{T}}{L}}_{=:N_u} U \,. \tag{7}$$

Analogously, equation (2) yields

$$\int\limits_V D_1 \mathrm{d}V = \int\limits_V \left(e_{111}^{T} \varepsilon_{11} + \epsilon_{11}^{\varepsilon,T} E_1 \right) \mathrm{d}V \tag{8}$$

$$\sum_{i=1}^{N} \int\limits_{(i-1)\frac{L}{N}}^{i\frac{L}{N}} \int\limits_A D_1 \mathrm{d}A \mathrm{d}x_1 = \sum_{i=1}^{N} \int\limits_{(i-1)\frac{L}{N}}^{i\frac{L}{N}} \int\limits_A \left(e_{111}^{T} \frac{\partial u}{\partial x_1} + \epsilon_{11}^{\varepsilon,T} E_1 \right) \mathrm{d}A \mathrm{d}x_1 \tag{9}$$

$$\underbrace{D_1 A N}_{=Q} \frac{L}{N} = e_{111}^{T} A \,(u(L) - u(0)) + \epsilon_{11}^{\varepsilon,T} A N \underbrace{\frac{L}{N} E_1}_{=U} \tag{10}$$

$$Q = \underbrace{\frac{A N e_{111}^{T}}{L}}_{=:N_u} (u(L) - u(0)) + \underbrace{\frac{A N^2 \epsilon_{11}^{\varepsilon,T}}{L}}_{=:C} U \,, \tag{11}$$

where Q is the total charge on the PZT stack. Equations (7) and (11) constitute the linear PZT stack model

$$F = k \Delta u - N_u U \tag{12}$$

$$Q = N_u \Delta u + C U \tag{13}$$

with $\Delta u = (u(L) - u(0))$ and the coefficients

$$N_u = \frac{A N e_{111}^{T}}{L} \,, \quad C = \frac{A N^2 \epsilon_{11}^{\varepsilon,T}}{L} \quad \text{and} \quad k = \frac{A c_{1111}^{E,T}}{L} \,, \tag{14}$$

Post-print version of the article: T. Müller, A. Kugi, G. Bachmaier, and M. Gerlich, "Modelling and identification of a piezoelectrically driven fuel injection control valve", *Mathematical and Computer Modelling of Dynamical Systems*, vol. 16, pp. 285–305, 2010. DOI: 10.1080/13873954.2010.502027

where k represents a stiffness, C a capacitance and N_u a coupling factor between mechanical and electrical variables. Obviously, all these coefficients depend on the temperature T and C and k are only constant for fixed values of the strain and the electric field. Therefore, the model (12), (13) is only accurate in small signal operation around the respective operating points. Thus, for large signal operation the model (12), (13) has to be extended or even replaced to account for the inherent nonlinear behaviour.

The structure of the stack model in (12) and (13) with two independent and two dependent variables motivates the use of port model representations, see, e.g., [13].

3.2. *Existing PSA models*

Even though Goldfarb and Celanovic [3] argue that their proposed model is completely phenomenological they implicitly use the linearized model (12) and (13) and extend it by an additional rate-independent Prandtl-Ishlinski hysteresis operator $H[Q]$ between the charge Q and the voltage U as can be seen in the signal flow for the material behaviour in Figure 3. The hysteresis between charge and voltage is motivated by experiments. In other publications, e.g. [9], the hysteresis is modelled between the voltage and the electric polarisation with the electric polarisation as an additional state in the model. Due to the fact that only one hysteresis operator

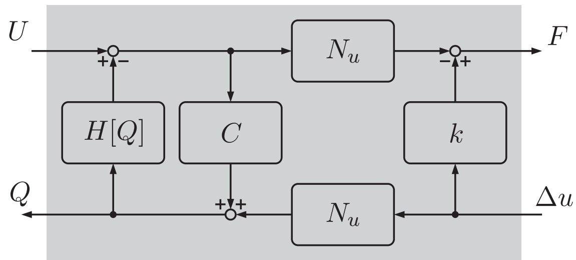

Figure 3. Signal flow of the material model proposed by Goldfarb et al. [3].

is used, the parametrization effort is much lower compared to other approaches. An adaptation to the temperature is not considered in [3].

Adrieaens et al. [4] refine the model by considering the distributed parameter structure of the actuator. Furthermore, they replace the Prandtl-Ishlinski hysteresis operator $H[Q]$ in Figure 3 by a Duhem hysteresis model [14], represented by a rate-independent differential equation with only three parameters. The use of differential equations for considering hysteretic effects further reduces the amount of parameters in the identification but deteriorates the model accuracy since it imposes a certain shape on the hysteresis by the structure of the differential equation. However, the model in [4] is only used for analyzing a modal representation but is not validated by means of measurements.

Wang [7] uses the material model of Goldfarb et al. and extends it for a parametrization over the temperature and adds experimental nonlinearities. The signal flow for the material behaviour is given in Figure 4, where in contrast to Figure 3 the input and output variables are interchanged. The various blocks in Figure 4 depend on the charge Q and the temperature T. For determining all the functions in Figure 4 a series of measurements under specific conditions has to be performed and approximated by suitable polynomials. The symmetry of $f_{FU}(T,Q)$ and $f_{QX}(T,Q)$ that is implied by the linearized constitutive equations is abandoned for a better adaptation of the system. The charge dependence is in

Post-print version of the article: T. Müller, A. Kugi, G. Bachmaier, and M. Gerlich, "Modelling and identification of a piezoelectrically driven fuel injection control valve", *Mathematical and Computer Modelling of Dynamical Systems*, vol. 16, pp. 285–305, 2010. DOI: 10.1080/13873954.2010.502027
The content of this post-print version is identical to the published paper but without the publisher's final layout or copy editing.

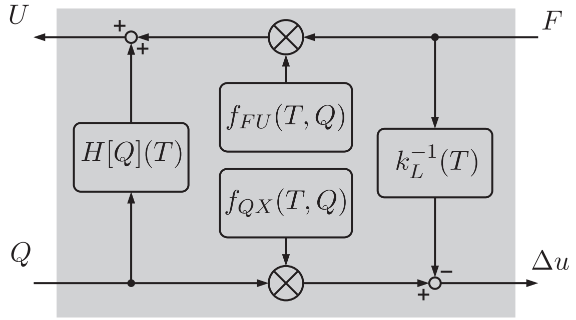

Figure 4. Signal flow for the material model by Wang [7].

parts only motivated by the experimental results. While $k_L(T)$ is essentially linear in the temperature, $f_{QX}(Q,T)$ and $f_{FU}(Q,T)$ have linear terms in Q, terms in T up to the order two and terms combining Q and T. Hysteresis is modeled by a differential equation approach with a memory for the hysteresis reversal points due to Dahl and Wilders [15] combined with several shaping functions for temperature adaptation. Creep is considered between charge and voltage by a linear second order filter. This highly parametrized model shows good results over a temperature range between -25°C and + 125°C. Yet the errors are not quantified.

Kuhnen [5] suggests an operator approach of the form

$$Q = \Gamma_e[U] + \Gamma_s[F] \tag{15}$$

$$\Delta u = \Gamma_a[U] + \Gamma_m[F]\,. \tag{16}$$

The operators Γ_i, $i \in \{a, e, m, s\}$, consist of a superposition operator for modelling static nonlinearities, a Prandtl-Ishlinski hysteresis operator for Γ_e, Γ_s and Γ_a and a creep operator for Γ_a and Γ_e. This approach is quite powerful and very accurate but the parametrization effort is extremely high. The invertibility of the used operators allows for the reconstruction of two arbitrary system variables when the other two variables are given. The parametrization requires the measurement of all system variables and the application of special input signals for identifying the hysteresis as well as special optimization procedures for a relatively high number of parameters. Changes in temperature and aging require a completely new parametrization. Actually, this is a general problem of all operator based models.

3.3. *PSA model used for system identification*

In this paper, the mathematical model of the PSA relies on the material model proposed by Goldfarb et al. [3] as depicted in Figure 3. In contrast to Wang [7] we aim at reducing the parametrization effort for temperature adaptation.

The structure of the PSA model is shown in Figure 5. The mass m_1 and the spring-damper combinations k_{gj}, b_{gj} with $j = 1, 2$ represent the mounting of the PSA as well as parts of the PSA itself. This includes the two bushings, the clamping ring, the housing of the PSA and the top plate. The total stiffness is determined by force-displacement measurements. The individual stiffness parameters k_{g1} and k_{g2} as well as the effective mass m_1 result from a Finite Element analysis of the respective components. For identification purposes the damping is set to zero. The PZT stack itself together with the tube shaped preloading spring and the top and bottom plate are included in the dashed box. The masses m_2 and m_3 comprise parts of the PZT stack mass, parts of the preloading spring mass and the top

Post-print version of the article: T. Müller, A. Kugi, G. Bachmaier, and M. Gerlich, “Modelling and identification of a piezoelectrically driven fuel injection control valve”, *Mathematical and Computer Modelling of Dynamical Systems*, vol. 16, pp. 285–305, 2010. doi: 10.1080/13873954.2010.502027

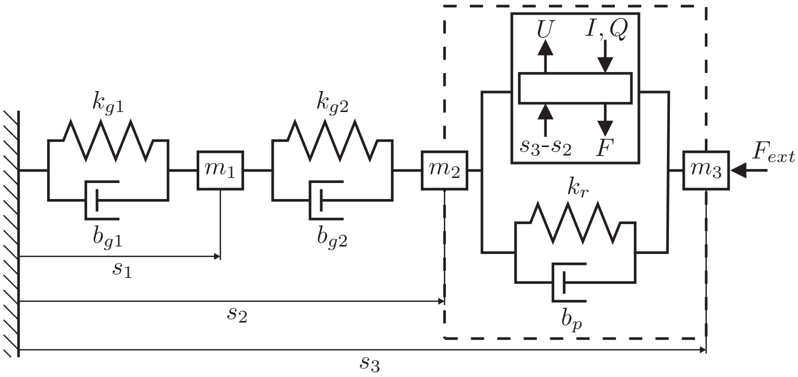

Figure 5. Structure of the mathematical model of the PSA with mounting.

and bottom plate masses, respectively. The material model is represented in the solid box, the preloading spring by the stiffness k_r and the material damping is considered by means of a viscous damping term with the coefficient b_p.

Utilizing the material model of Figure 3 (see also (12) and (13)) for $\Delta u = s_3 - s_2$, the equations of motion read as

$$m_1\ddot{s}_1 = -k_{g1}s_1 - b_{g1}\dot{s}_1 + k_{g2}(s_2 - s_1) + b_{g2}(\dot{s}_2 - \dot{s}_1) \tag{17}$$

$$m_2\ddot{s}_2 = -k_{g2}(s_2 - s_1) - b_{g2}(\dot{s}_2 - \dot{s}_1) + \left(k_p + \frac{N_u^2}{C}\right)(s_3 - s_2) + b_p(\dot{s}_3 - \dot{s}_2) - \frac{N_u}{C}Q \tag{18}$$

$$m_3\ddot{s}_3 = -\left(k_p + \frac{N_u^2}{C}\right)(s_3 - s_2) + \frac{N_u}{C}Q - b_p(\dot{s}_3 - \dot{s}_2) - F_{ext} \tag{19}$$

with $k_p = k + k_r$ as the sum of the material stiffness k, cf. (14), and the preloading spring stiffness k_r and F_{ext} as the external force acting on the PSA. Furthermore, the output voltage U is given by the relation

$$U = -\frac{N_u}{C}(s_3 - s_2) + \frac{1}{C}Q + H[Q]\,. \tag{20}$$

With the charge Q and the external force F_{ext} as inputs the system (17)-(20) possesses the structure of a Wiener model with a linear dynamics and a hysteretic nonlinearity $H[Q]$ in the output equation [16]. Note that, if the voltage U is the input a so called Hammerstein model structure, i.e. a series connection of a hysteretic input nonlinearity and a linear dynamics, is obtained. In this case the nonlinearity at the input may be exactly compensated by inverting the nonlinear input operator, see, e.g., [17].

For adapting the model to temperature variations the following assumptions are made, which are mainly based on experimental results.

- The term $\left(k_p + \frac{N_u^2}{C}\right)$ in (18) represents the total PSA stiffness with the combined material and preloading stiffness k_p and an additional stiffness due to the piezoelectric effect. Wang [7] reports that the measured total stiffness of the actuator varies only slightly between about 118 N/μm and 126 N/μm over a temperature range of -25°C to 125°C. With the additional assumption that the material

Post-print version of the article: T. Müller, A. Kugi, G. Bachmaier, and M. Gerlich, "Modelling and identification of a piezoelectrically driven fuel injection control valve", *Mathematical and Computer Modelling of Dynamical Systems*, vol. 16, pp. 285–305, 2010. DOI: 10.1080/13873954.2010.502027

stiffness k, cf. (14), does not depend on the temperature we assess the factor

$$k_s = \frac{N_u^2}{C} \tag{21}$$

to be also constant over temperature. This results in a fixed relation between the two temperature dependent parameters N_u and C and in a temperature independent value for k_p.

- For the specific class of input signals being used in the identification procedure of Section 4, the rising branch of the hysteresis operator $H[Q]$ in the charging phase is approximated by the time evolution of the term $R(N_u)I$. This will be demonstrated in more detail in the following section. The relation

$$R(N_u) = R_{0a}e^{-R_{0b}N_u} \tag{22}$$

with the constant coefficients R_{0a} and R_{0b} is a result of the parameter identification described later on.
- For a better model adaptation the damping coefficient b_p is related to the parameter N_u by $b_p = R_b N_u^2$ with a constant value for R_b.

Summarizing, the mathematical model of the PSA with mounting can then be described in the form of a linear differential equation[1]

$$\dot{\mathbf{x}} = \mathbf{A}\mathbf{x} + \mathbf{B}\mathbf{u} \tag{23}$$

$$y = \mathbf{c}^T\mathbf{x} + \mathbf{d}^T\mathbf{u} \tag{24}$$

where $\mathbf{x} = \left[s_1 \; \dot{s}_1 \; s_2 \; \dot{s}_2 \; s_3 \; \dot{s}_3 \; Q \right]^T$ denotes the state, $\mathbf{u} = \left[I \; F_{ext} \right]^T$ refers to the input, $y = U$ is the output and

$$\mathbf{A} = \begin{bmatrix} 0 & 1 & 0 & 0 & 0 & 0 & 0 \\ -\frac{k_{g2}+k_{g1}}{m_1} & -\frac{b_{g2}+b_{g1}}{m_1} & \frac{k_{g2}}{m_1} & \frac{b_{g2}}{m_1} & 0 & 0 & 0 \\ 0 & 0 & 0 & 1 & 0 & 0 & 0 \\ \frac{k_{g2}}{m_2} & \frac{b_{g2}}{m_2} & -\frac{k_{g2}+k_p+k_s}{m_2} & -\frac{b_{g2}+b_p}{m_2} & \frac{k_p+k_s}{m_2} & \frac{b_p}{m_2} & -\frac{1}{m_2}\frac{k_s}{N_u} \\ 0 & 0 & 0 & 0 & 0 & 1 & 0 \\ 0 & 0 & \frac{k_p+k_s}{m_3} & \frac{b_p}{m_3} & -\frac{k_p+k_s}{m_3} & -\frac{b_p}{m_3} & \frac{1}{m_3}\frac{k_s}{N_u} \\ 0 & 0 & 0 & 0 & 0 & 0 & 0 \end{bmatrix}, \quad \mathbf{B} = \begin{bmatrix} 0 & 0 \\ 0 & 0 \\ 0 & 0 \\ 0 & 0 \\ 0 & 0 \\ 0 & -\frac{1}{m_3} \\ 1 & 0 \end{bmatrix},$$

$$\mathbf{c}^T = \left[0 \; 0 \; \frac{k_s}{N_u} \; 0 \; -\frac{k_s}{N_u} \; 0 \; \frac{k_s}{N_u^2} \right], \quad \mathbf{d}^T = \left[R(N_u) \; 0 \right]$$

with $b_p = R_b N_u^2$ and $R(N_u) = R_{0a}e^{-R_{0b}N_u}$ due to (22). The advantage of this model compared to other approaches known from the literature is that the adaptation to temperature variation is solely done via one temperature dependent parameter N_u and no complex hysteresis model has to be considered. The validity of the model is limited to a specific class of input signals in the charging phase of the PSA. However, this turns out to be sufficient for the identification of the idle stroke value as will be shown in Section 5.

[1]Note that in this formulation the current I and not the charge Q is used as the input to the system.

Post-print version of the article: T. Müller, A. Kugi, G. Bachmaier, and M. Gerlich, “Modelling and identification of a piezoelectrically driven fuel injection control valve”, *Mathematical and Computer Modelling of Dynamical Systems*, vol. 16, pp. 285–305, 2010. DOI: 10.1080/13873954.2010.502027

Table 1. Nominal PSA parameters

m_1 $[10^{-3}\text{kg}]$	m_2 $[10^{-3}\text{kg}]$	m_3 $[10^{-3}\text{kg}]$	k_p $[10^6\text{N/m}]$	k_{g1} $[10^6\text{N/m}]$	k_{g2} $[10^6\text{N/m}]$	k_s $[10^6\text{N/m}]$
27.764	6.5	9.9	62.15	456.2	331.66	118.72
b_{g1} [N/ms]	b_{g2} [N/ms]	R_b $[\text{V}^2/\text{msN}]$	R_{0a} [Ω]	R_{0b} $[V/N]$	N_u $[N/V]$	
0	0	3.33	1764.4	0.4558	$15\ldots21$	

The mounting parameters m_1, k_{g1}, k_{g2}, b_{g1} and b_{g2} are identified by means of Finite Element analysis and measurement results. The remaining masses are determined by weighing the individual components of the system and by allocating them to the model masses m_2 and m_3. All other parameters are obtained by nonlinear optimization based on the measurements of the voltage and displacement signals for different temperatures.

For this let us assume that $y(\mathbf{x}_0, I(t); \mathbf{p}; N_u; R)$ and $x_5(\mathbf{x}_0, I(t); \mathbf{p}; N_u; R)$ denote the time evolution of the voltage $U(t)$ and the bottom plate displacement $s_3(t)$ of the mathematical model (23), (24) for the initial condition $\mathbf{x}(0) = \mathbf{x}_0$, the current input $I(t)$, the external force $F_{ext} = 0\,\text{N}$, the parameter vector $\mathbf{p} = \left[k_p,\, k_s,\, R_b\right]^T$ and the temperature dependent parameters N_u and R for a fixed temperature T. Now the parameter vector $\mathbf{p}$ and the functional dependence $N_u(T)$ and $R(T)$ are determined by solving the optimization problem

$$
\begin{aligned}
\min_{\mathbf{p}, N_{u,j}, R_j, j=1,\ldots,M} \quad & \sum_{j=1}^{M} \int_0^{t_1} \left| U_{m,j}(t) - y\left(\mathbf{x}_0, I(t); \mathbf{p}; N_{u,j}; R_j\right) \right| \\
& + \gamma \left| s_{3m,j}(t) - x_5\left(\mathbf{x}_0, I(t); \mathbf{p}; N_{u,j}; R_j\right) \right| \mathrm{d}t \qquad (25) \\
\text{s. t.} \quad & \dot{\mathbf{x}} = \mathbf{A}\left(\mathbf{p}; N_{u,j}\right)\mathbf{x} + \mathbf{B}\mathbf{u}\,, \quad \mathbf{x}(0) = \mathbf{x}_0 \\
& y = \mathbf{c}^T\left(\mathbf{p}; N_{u,j}\right)\mathbf{x} + \mathbf{d}\left(\mathbf{p}; R_j\right)\mathbf{u}\,,
\end{aligned}
$$

where $U_{m,j}(t)$ and $s_{3m,j}(t)$, $j = 1, \ldots, M$ are the measured time evolutions of the voltage and the bottom plate displacement for a fixed temperature T_j and thus fixed parameters $N_{u,j}$ and R_j.

The cost function of the optimization problem (25) is an integral formulation of the absolute voltage and deflection error between measurement and simulation. For scaling the two different errors, the deflection error is weighted by the factor $\gamma > 0$. The absolute error integral formulation is chosen since it has in general a higher gradient close to the optimum than a quadratic error integral formulation [18]. For solving the optimization problem the 'fmincon'-command in MATLAB is used. The gradient of the cost function is not provided for the optimization. For improving the convergence, parameter constraints are included in the optimization problem.

The values of the parameter vector resulting from this optimization are given in Table 1. The functional dependence of the parameters N_u and R on the temperature T as well as the relation $R(N_u)$ are displayed in Figure 6. The relation $N_u(T)$ is approximated by a linear function, the relation $R(T)$ by an exponential function and $R(N_u)$ as a combination of the relations $N_u(T)$ and $R(T)$ according to (22).

Thus the mathematical model (23), (24) is fully parametrized and can be utilized for adaptation purposes in the next section.

Post-print version of the article: T. Müller, A. Kugi, G. Bachmaier, and M. Gerlich, "Modelling and identification of a piezoelectrically driven fuel injection control valve", *Mathematical and Computer Modelling of Dynamical Systems*, vol. 16, pp. 285–305, 2010. DOI: 10.1080/13873954.2010.502027

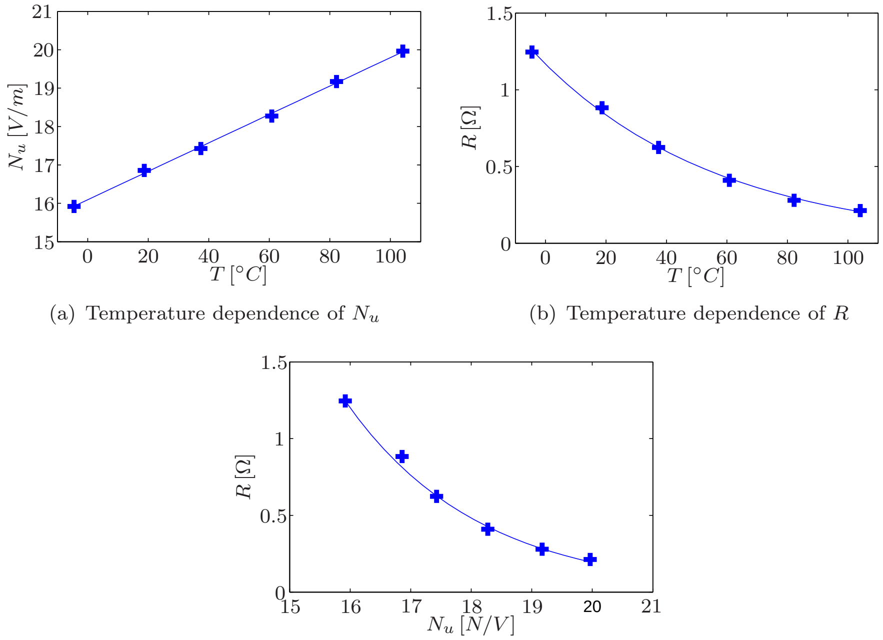

(a) Temperature dependence of N_u

(b) Temperature dependence of R

(c) Relation $R(N_u)$

Figure 6. Optimization results of $N_u(T)$ and $R(T)$ for different temperatures and the relation $R(N_u)$ with approximations.

4. Model adaptation

In the practical application only the voltage signal $U(t)$ is measurable. For this reason, the adaptation of the mathematical model (23), (24) to temperature variations and changes of the parameters in the series production is performed by solving the optimization problem

$$\begin{aligned} &\min_{N_u} \int_0^{t_1} \left| U_m(t) - y\left(\mathbf{x}_0, I(t); N_u\right)\right| \mathrm{d}t \\ &\text{s. t.} \quad \dot{\mathbf{x}} = \mathbf{A}\left(N_u\right)\mathbf{x} + \mathbf{B}\mathbf{u}\,, \quad \mathbf{x}\left(0\right) = \mathbf{x}_0 \\ &\qquad\quad y = \mathbf{c}^T\left(N_u\right)\mathbf{x} + \mathbf{d}\left(N_u\right)\mathbf{u} \end{aligned} \tag{26}$$

where $U_m(t)$ denotes the measured time evolution of the output voltage and $y\left(\mathbf{x}_0, I(t); N_u\right)$ refers to the time evolution of the simulated output voltage of the mathematical model (23), (24) with $R(N_u)$ due to (22), the initial condition $\mathbf{x}\left(0\right) = \mathbf{x}_0$, the current input $I(t)$, the external force $F_{ext} = 0\,\mathrm{N}$ and the parameter N_u. Except for N_u all other parameters are fixed to their nominal values according to Table 1. Figure 7 depicts the results for a PSA which is subject to different temperatures in a range from 0°C to 100°C. The vertical line at $t = 170\mu\mathrm{s}$ in Figure 7(a) refers to the time t_1, i.e. the end time of the optimization interval, see also (26). Since we are primarily interested in the idle stroke detection, several investigations have shown that the charging phase period turns out to be a good choice for the optimization interval. It can be seen in Figure 7 that the changes due to temperature variations can be adapted in an excellent way by means of the proposed method. The voltage error turns out to be less than $\pm 2\mathrm{V}$, see Figure 7(c), and the displacement error is smaller than $\pm 0.7\mu\mathrm{m}$, see Figure 7(d).

Post-print version of the article: T. Müller, A. Kugi, G. Bachmaier, and M. Gerlich, “Modelling and identification of a piezoelectrically driven fuel injection control valve”, *Mathematical and Computer Modelling of Dynamical Systems*, vol. 16, pp. 285–305, 2010. DOI: 10.1080/13873954.2010.502027

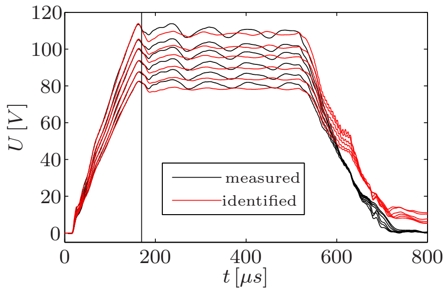

(a) Voltage

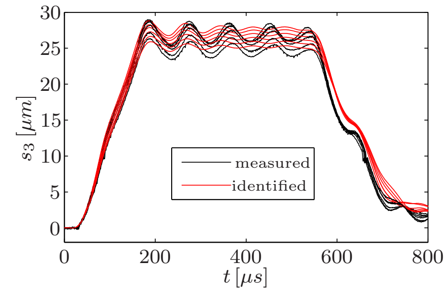

(b) Displacement of the bottom plate

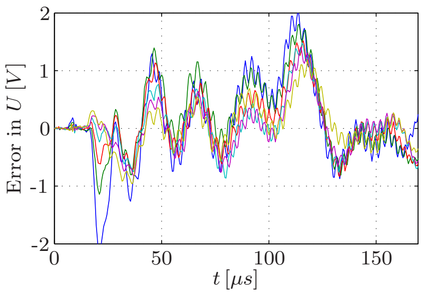

(c) Voltage error

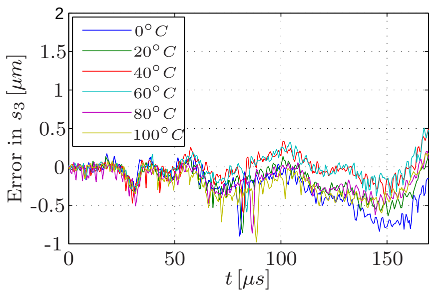

(d) Displacement error of the bottom plate

Figure 7. Adaptation to different temperatures by means of the voltage and the current signal: Voltage, displacement and corresponding errors.

For checking the robustness of the PSA model with respect to parameter variations due to series production several actuators are adapted by means of the parameter N_u solving the optimization problem (26). Figure 8 presents the results of the adaptation of ten different PSAs with a similar history at room temperature. The voltage and displacement errors are for all PSAs basically the same. Furthermore, the identified parameters N_u are very close together as shown in detail in Figure 8(c). However, this proves the feasibility of the proposed method to adapt the mathematical model (23), (24) to changing temperatures and to changing parameters in series production.

5. Idle stroke detection

For the model based identification of the idle stroke value the PSA model has to be extended by a mechanical model for the control valve. This extended model is then used for combined identification of the coupling parameter N_u and the idle stroke value.

5.1. *Separation between model errors and voltage change due to a different idle stroke value*

In order to quantify the change in the output voltage due to changes in the idle stroke value the difference in the measured voltage signal with different idle stroke values is given in Figure 9. The three thin curves are the voltage differences $\Delta U_j(t) = U_{L_{h1}}(t) - U_{L_{hj}}(t)$, $j = 2, 3, 4$ for increasing idle stroke values $L_{h1} < L_{h2} < L_{h3} < L_{h4}$. The difference between neighboring idle stroke values is between 2.5μm and 3μm. It can be seen that the time evolutions $\Delta U_2(t)$, $\Delta U_3(t)$ and $\Delta U_4(t)$ are almost identical until a collision between the bottom plate of the

Post-print version of the article: T. Müller, A. Kugi, G. Bachmaier, and M. Gerlich, "Modelling and identification of a piezoelectrically driven fuel injection control valve", *Mathematical and Computer Modelling of Dynamical Systems*, vol. 16, pp. 285–305, 2010. DOI: 10.1080/13873954.2010.502027
The content of this post-print version is identical to the published paper but without the publisher's final layout or copy editing.

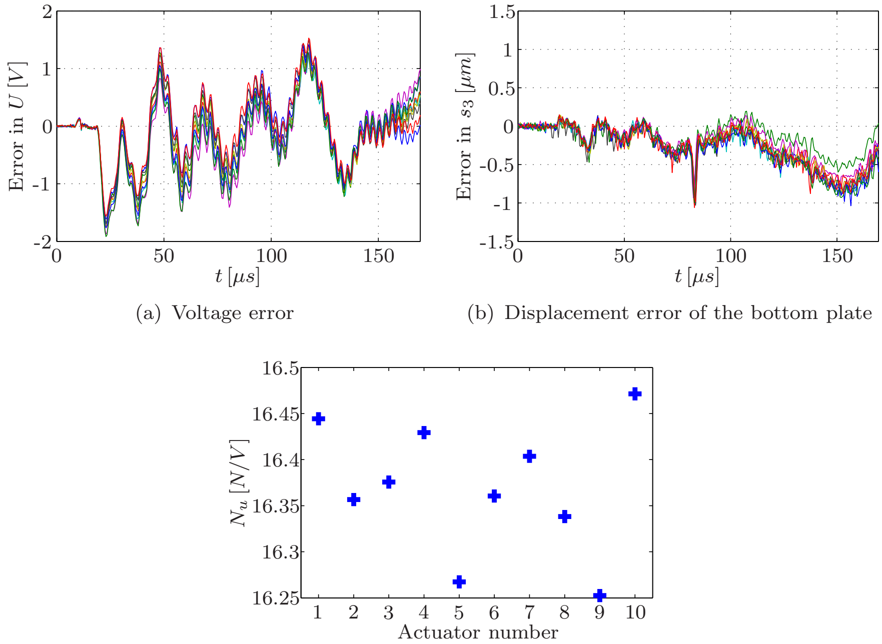

(a) Voltage error

(b) Displacement error of the bottom plate

(c) Parameter N_u for each actuator.

Figure 8. Adaptation of different PSAs at room temperature.

PSA and the piston occurs. The error between the measured voltage and the simulated voltage of the adapted model of a PSA without control valve is shown by the thick curve in Figure 9. This error cancels out in the voltage difference signals $\Delta U_j(t)$, $j = 2, 3, 4$. However, for detecting an idle stroke value from a single measurement both effects are superimposed. The voltage errors are clearly distinguishable in their shape but since they are in the same range the accuracy of the model is a crucial point for a successful identification. The difference between the voltage signals for different idle stroke values L_{hj} increases with the force that keeps the control valve closed. In the experiments this is only the force exerted by the control valve spring that is preloaded with a force $F_{open} = 28$N. Under real operating conditions the fuel pressure force increases this force up to several hundred N.

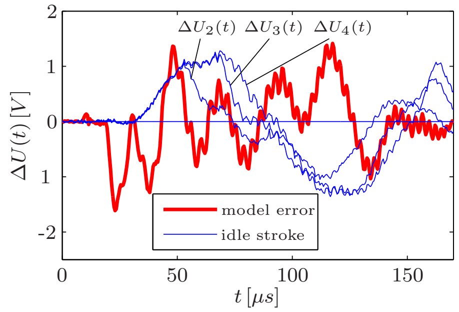

Figure 9. Voltage signal difference due to the model error and due to the different idle stroke values.

Post-print version of the article: T. Müller, A. Kugi, G. Bachmaier, and M. Gerlich, “Modelling and identification of a piezoelectrically driven fuel injection control valve”, *Mathematical and Computer Modelling of Dynamical Systems*, vol. 16, pp. 285–305, 2010. doi: 10.1080/13873954.2010.502027
The content of this post-print version is identical to the published paper but without the publisher’s final layout or copy editing.

Table 2. Parameters of the control valve mechanics

m_4	k_f	k_{v1}	k_{v2}	s_p	b_f	b_v	F_{open}	L_h
$[10^{-3}\text{kg}]$	$[10^3\text{N/m}]$	$[10^6\text{N/m}]$	$[10^6\text{N/m}]$	$[10^{-6}\text{m}]$	[N/ms]	[N/ms]	[N]	$[10^{-6}\text{m}]$
1.2	30	13.2	578.8	2.04	0	93.4	28	$-2\ldots10$

5.2. *Mechanical model of the control valve*

The mechanical model of the control valve determines the time evolution of the load force F_{ext}, see (19), on the PSA when the PSA gets into contact with the valve piston. The mechanical load causes a change in the time evolution of the voltage of the PSA. Since both, the model error and the change in the voltage due to the mechanical load, are in the same range (see Figure 9) the accuracy of the mechanical model of the control valve is essential for the idle stroke detection.

A hybrid system consisting of an automaton with three discrete states referring to three different time continuous subsystems Σ_i, $i = 1, 2, 3$, is used for describing the valve mechanics. For the model description we assume subsystem Σ_1 as the initial location imposing the zero initial conditions for the continuous state. In subsystem Σ_1 (Figure 10(a)) there is no contact between the PSA and the piston. Subsystem Σ_2 (Figure 10(b)) describes the situation when the PSA bottom plate is already in contact with the valve piston ($s_3(t) \leq L_h$) but the force on the valve piston is smaller than the preload force F_{open}. Subsystem Σ_3 (Figure 10(c)) is active when this force exceeds the preload force. In subsystem Σ_3 the preloading spring is modeled by a linear spring with $F_f(s) = k_f s$ and for completeness a viscous damper with the coefficient b_f is included. The switching between these three subsystems is performed according to the automaton given in Figure 12.

One important modelling issue is the contact between the PSA bottom plate and the valve piston. Allowing only limited complexity of the model leads to two possible modelling approaches. In the first approach, the collision is modeled by means of the conservation of momentum and the coefficient of restitution is used to quantify the energy loss as described in many mechanics books, see, e.g., [19]. Thereby, it is assumed that the collision takes place instantaneously compared to the system dynamics and sampling time. In our application, however, this assumption does not hold true since the sampling time of $0.5\,\mu$s is extremely small. The second approach considers the contact by means of a spring and, if energy dissipation is included, a viscous damper. The damper leads to a discontinuity in the vector field when switching between subsystem Σ_1 and Σ_2. Nevertheless, the well-posedness of the system is guaranteed in this case, see, e.g., [20, 21].

For a better adaptation of the contact process a piecewise linear spring $F_v(s)$ according to Figure 11 is used. While for the contact a smaller stiffness k_{v1} is useful, the higher stiffness k_{v2} accounts for the material stiffness. The switching between the two stiffness parameters is given by the compression length s_p. For the clarity of presentation, $F_v(s)$ is included as a function and not as an additional discrete state in the automaton of Figure 12. The coefficient of the viscous damper is denoted by b_v in Figure 10.

When switching from subsystem Σ_2 to subsystem Σ_3, $\dot{s}_4$ is set equal to $\dot{s}_3$ at the switching point. This results in an almost in phase movement of the masses m_3 and m_4 when the control valve opens and avoids oscillations in the simulated valve plunger position s_4. The mass m_4 represents the combined valve plunger and valve piston mass. The switching conditions from subsystem Σ_3 to subsystem Σ_2 and from subsystem Σ_2 to subsystem Σ_1 can be inferred from Figure 12. However, since this is not relevant for the idle stroke detection we will not go into further details here. The parameters of the control valve mechanics are summarized in Table 2. The values are determined experimentally.

Post-print version of the article: T. Müller, A. Kugi, G. Bachmaier, and M. Gerlich, "Modelling and identification of a piezoelectrically driven fuel injection control valve", *Mathematical and Computer Modelling of Dynamical Systems*, vol. 16, pp. 285–305, 2010. DOI: 10.1080/13873954.2010.502027

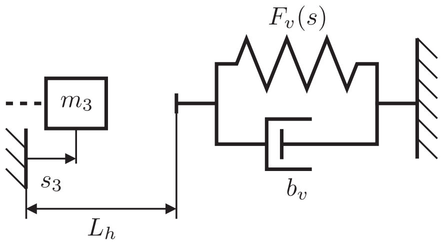

(a) Subsystem Σ_1

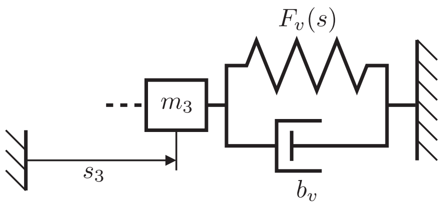

(b) Subsystem Σ_2

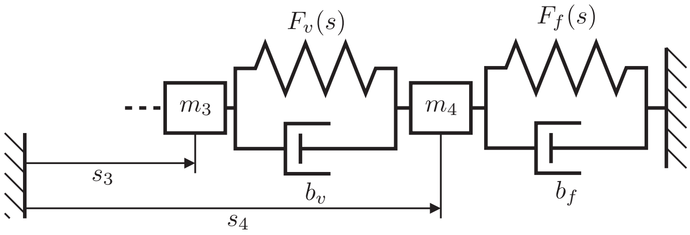

(c) Subsystem Σ_3

Figure 10. Mechanical model of the switching process.

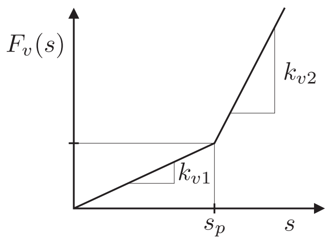

Figure 11. Contact stiffness force $F_v(s)$ between PSA bottom plate and valve piston.

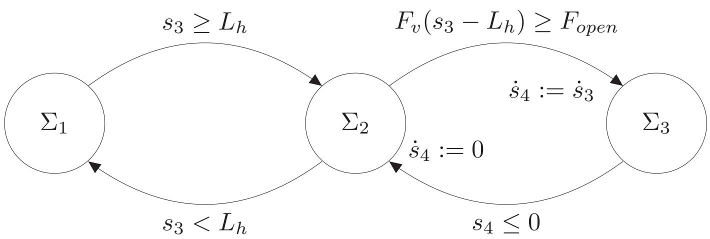

Figure 12. Automaton for the hybrid system describing the valve mechanics.

The mathematical model (23), (24) extended by the valve mechanics, see Figure 10 – Figure 12, takes the form

$$\Sigma_i : \begin{cases} \dot{\mathbf{x}}_\mathbf{e} = \mathbf{A}_{\mathbf{e},i}\left(N_u\right)\mathbf{x}_\mathbf{e} + \mathbf{B}_{\mathbf{e},i}\mathbf{u} + \mathbf{b}_{\mathbf{e},i}L_h\,, \quad \mathbf{x}_\mathbf{e}\left(0\right) = \mathbf{x}_{\mathbf{e}0} \\ y \quad = {\mathbf{c}_\mathbf{e}}^T\left(N_u\right)\mathbf{x}_\mathbf{e} + \mathbf{d}_\mathbf{e}\left(N_u\right)\mathbf{u} \end{cases} \tag{27}$$

with the hybrid automaton according to Figure 12 determining the switching events from subsystem Σ_j to Σ_i and the re-initialization of the continuous states $\mathbf{x}_\mathbf{e}$ when a switching occurs. The extended continuous state vector is given by $\mathbf{x}_\mathbf{e} = \left[s_1\ \dot{s}_1\ s_2\ \dot{s}_2\ s_3\ \dot{s}_3\ Q\ s_4\ \dot{s}_4\right]^T$, the input reads as $\mathbf{u} = [I, F_{open}]^T$ with F_{open}=const. and the output y corresponds to the voltage U.

Now, the combination of the adaptation to changes in the temperature and the

Post-print version of the article: T. Müller, A. Kugi, G. Bachmaier, and M. Gerlich, “Modelling and identification of a piezoelectrically driven fuel injection control valve”, *Mathematical and Computer Modelling of Dynamical Systems*, vol. 16, pp. 285–305, 2010. DOI: 10.1080/13873954.2010.502027

detection of an idle stroke value can again be formulated as an optimization problem

$$\min_{N_u, L_h} J_{Ue}(N_u, L_h)\,, \qquad J_{Ue}(N_u, L_h) = \int_0^{t_1} |U_m(t) - y\left(\mathbf{x_{e0}}, I(t), F_{open}; N_u; L_h\right)| \,\mathrm{d}t$$
$$\text{s.t. (27) and Fig. 12} \tag{28}$$

Here $U_m(t)$ is the measured voltage signal and $y\left(\mathbf{x_{e0}}, I(t), F_{open}; N_u; L_h\right)$ denotes the simulated time-evolution of the output voltage of the hybrid automaton due to Figure 12 with Σ_i, $i = 1, 2, 3$ from (27), the initial condition $\mathbf{x_e}(0) = \mathbf{x_{e0}}$, the current input $I(t)$, the constant spring preload force F_{open} and the coupling parameter N_u as well as the idle stroke value L_h. This optimization problem can be solved by means of the previously described optimization method. Simulation results have shown that the effect of a change in the parameters N_u and L_h can be clearly distinguished in the model output $y = U$. Therefore, at least local convergence of the optimization can be assumed and is demonstrated in the following by means of measurement results for different temperatures.

5.3. *Idle stroke detection at different temperatures*

In this section, the detection of different idle stroke values L_h by means of the optimization approach (28) is shown at room temperature and at 100°C.

First let us consider the measurements at room temperature. The difference between the measured signals and the signals of the adapted system by N_u and L_h are presented in Figure 13. The voltage error for all idle stroke values is almost identical, see Figure 13(c). Also the error of the valve plunger position s_4 is less than $1\,\mu$m in the charging phase. A wrong idle stroke value leads to a constant bias in the estimated position s_4. In order to get a more accurate identification result for the idle stroke the signal range for the optimization is diminished, since model errors tend to get larger with time. The end of the optimization interval at $t_1 = 100\,\mu$s is indicated by the vertical line in Figure 13(a) and 13(c).

The contour plots of the corresponding cost function $J_{Ue}(N_u, L_h)$ over the parameters N_u and L_h for the measurements with different idle stroke values from Figure 13 are given in Figure 14. The adapted parameters N_u and L_h are determined by the minimum of the cost function. Even though the gradient of the cost function around the minima is relatively small, the minima can be clearly distinguished for the different idle stroke values. Negative idle stroke values L_h refer to a compression of the valve piston. In such a case the automaton in Figure 12 starts from subsystem Σ_2 or Σ_3 with nonzero initial conditions. When the initial subsystem is Σ_3 the optimization problem (28) is no longer feasible, which is why a lower bound for the parameter L_h is imposed.

Next the identification method is applied to measurements at 100°C. The results in Figure 15 and 16 are similar to those at room temperature. Just the largest idle stroke seems to have a slightly larger deviation.

5.4. *Idle stroke detection with different actuators*

Moreover, the system adaptation by means of the idle stroke value L_h and the coupling parameter N_u is performed for ten different actuators at room temperature. In order to avoid a large number of figures the results are summed up in Table 3. For each actuator the identified coupling parameter N_u, the identified idle stroke

Post-print version of the article: T. Müller, A. Kugi, G. Bachmaier, and M. Gerlich, "Modelling and identification of a piezoelectrically driven fuel injection control valve", *Mathematical and Computer Modelling of Dynamical Systems*, vol. 16, pp. 285–305, 2010. DOI: 10.1080/13873954.2010.502027

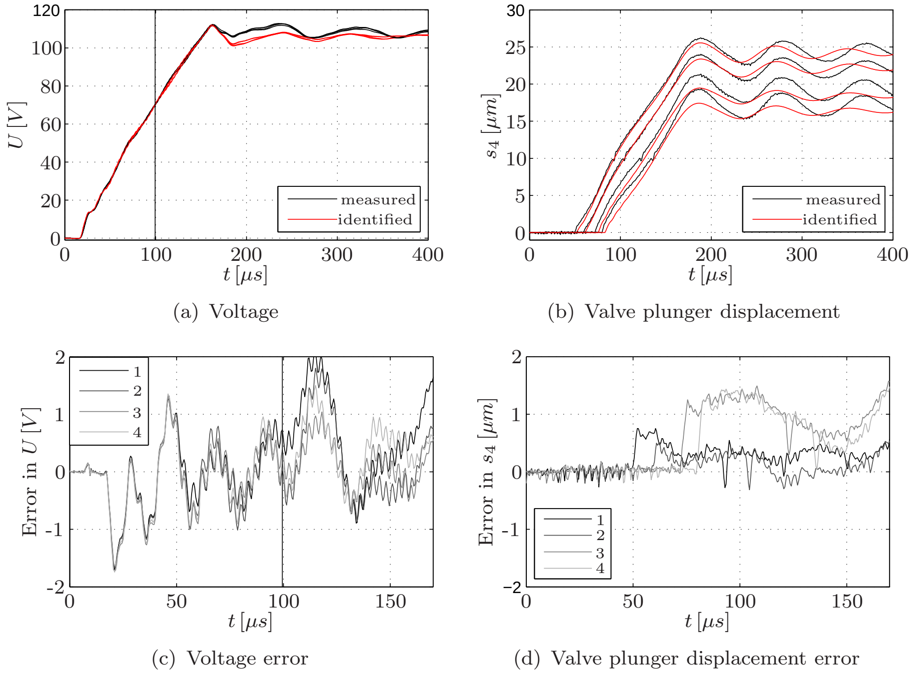

Figure 13. Results of the idle stroke detection at room temperature: signals and errors.

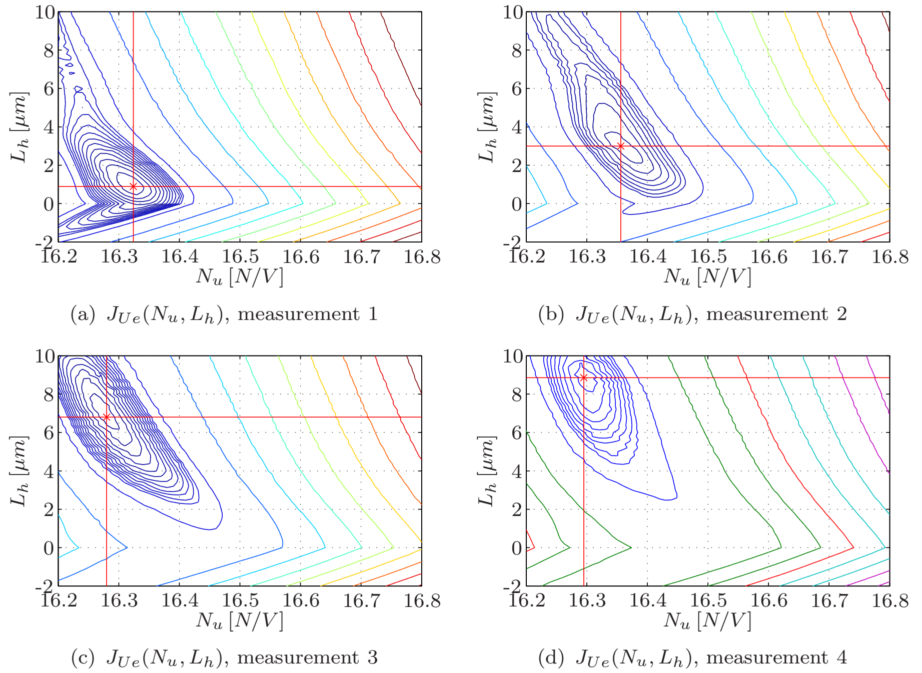

Figure 14. Results of the idle stroke detection at room temperature: contour plots of the cost function $J_{Ue}(N_u, L_h)$.

value L_h and the cost function minimum value are given. Since the idle stroke value cannot be measured directly, the mean plunger displacement $s_{4,s}$ between 215 μs and 490 μs (plateau range) is given in the table for comparing the measurements with the adapted simulation results. The range used for the optimization is again from 0 to 100 μs.

The error of the mean plunger displacement between measurement and adapted

Post-print version of the article: T. Müller, A. Kugi, G. Bachmaier, and M. Gerlich, "Modelling and identification of a piezoelectrically driven fuel injection control valve", *Mathematical and Computer Modelling of Dynamical Systems*, vol. 16, pp. 285–305, 2010. DOI: 10.1080/13873954.2010.502027
The content of this post-print version is identical to the published paper but without the publisher's final layout or copy editing.

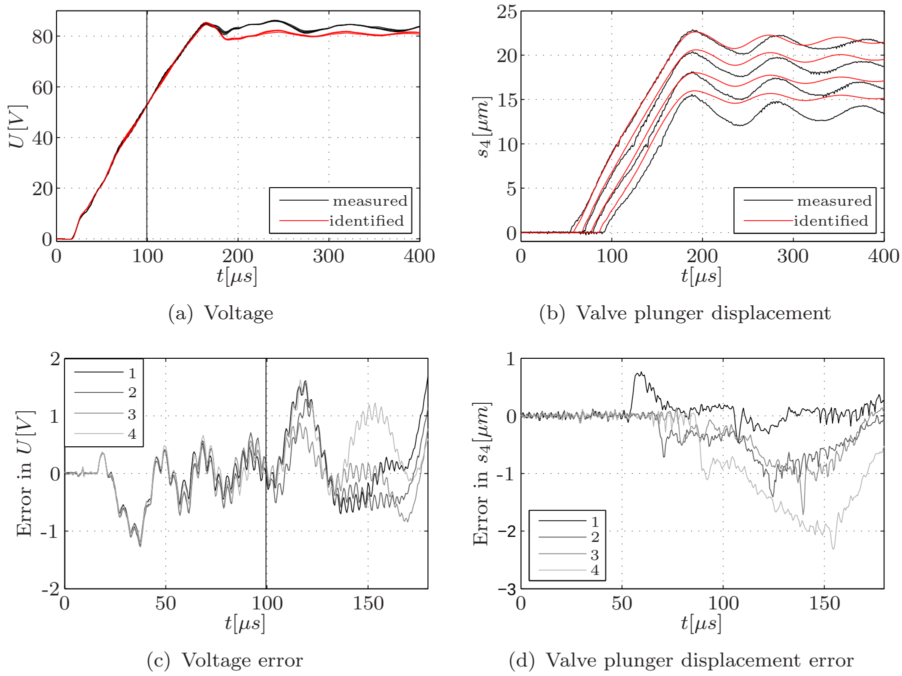

(a) Voltage
(b) Valve plunger displacement
(c) Voltage error
(d) Valve plunger displacement error

Figure 15. Result of the idle stroke detection at 100°C: signals and errors.

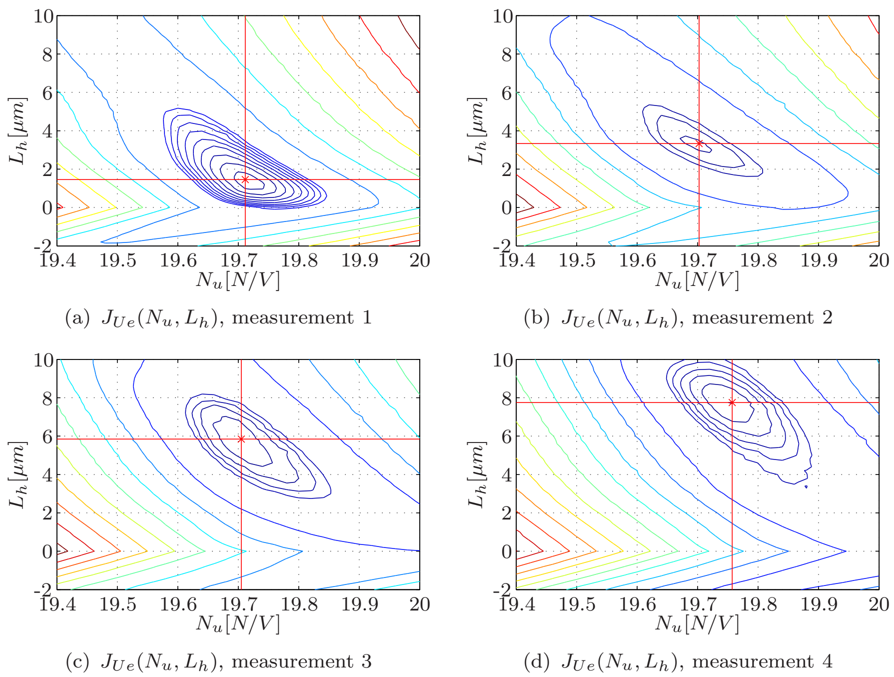

(a) $J_{Ue}(N_u, L_h)$, measurement 1
(b) $J_{Ue}(N_u, L_h)$, measurement 2
(c) $J_{Ue}(N_u, L_h)$, measurement 3
(d) $J_{Ue}(N_u, L_h)$, measurement 4

Figure 16. Results of the idle stroke detection at 100°C: contour plots of the cost function $J_{Ue}(N_u, L_h)$.

simulation is for all measurements with different PSAs and idle stroke values between -0.56 and +1.09μm. An error in the idle stroke value leads exactly to the same error in the mean plunger displacement provided that other stationary model errors can be neglected. Therefore, one can conclude that the accuracy of the proposed idle stroke detection method lies within the same range.

Post-print version of the article: T. Müller, A. Kugi, G. Bachmaier, and M. Gerlich, "Modelling and identification of a piezoelectrically driven fuel injection control valve", *Mathematical and Computer Modelling of Dynamical Systems*, vol. 16, pp. 285–305, 2010. DOI: 10.1080/13873954.2010.502027

Table 3. Identification results PSA No. 1 to 10.

PSA No. 1					
meas	N_u [N/V]	L_h [μm]	$s_{4,s}$ [μm] meas	$s_{4,s}$ [μm] sim	Cost [μVs]
1	16.39	0.6	24.89	24.50	51.18
2	16.37	2.5	22.04	22.59	46.61
3	16.35	6.8	18.88	18.40	42.84
4	16.37	8.4	16.75	16.71	46.08

PSA No. 2					
meas	N_u [N/V]	L_h [μm]	$s_{4,s}$ [μm] meas	$s_{4,s}$ [μm] sim	Cost [μVs]
1	16.32	0.9	24.24	24.14	43.24
2	16.35	3.0	21.99	22.10	48.43
3	16.28	6.8	19.17	18.34	43.47
4	16.30	8.9	17.06	16.31	46.90

PSA No. 3					
meas	N_u [N/V]	L_h [μm]	$s_{4,s}$ [μm] meas	$s_{4,s}$ [μm] sim	Cost [μVs]
1	16.38	0.6	25.18	24.44	52.42
2	16.34	3.6	21.39	21.45	50.30
3	16.28	6.8	19.19	18.38	48.25
4	16.31	8.6	16.92	16.55	54.90

PSA No. 4					
meas	N_u [N/V]	L_h [μm]	$s_{4,s}$ [μm] meas	$s_{4,s}$ [μm] sim	Cost [μVs]
1	16.44	0.8	24.70	24.15	55.84
2	16.37	3.6	21.91	21.39	50.94
3	16.37	4.7	19.74	20.32	49.00
4	16.38	8.4	17.01	16.63	56.35

PSA No. 5					
meas	N_u [N/V]	L_h [μm]	$s_{4,s}$ [μm] meas	$s_{4,s}$ [μm] sim	Cost [μVs]
1	16.37	0.8	24.70	24.18	52.15
2	16.31	3.4	21.93	21.68	50.25
3	16.32	5.2	19.80	19.90	49.40
4	16.32	8.4	16.99	16.61	48.10

PSA No. 6					
meas	N_u [N/V]	L_h [μm]	$s_{4,s}$ [μm] meas	$s_{4,s}$ [μm] sim	Cost [μVs]
1	16.41	0.8	24.38	24.22	49.17
2	16.37	3.2	21.79	21.82	50.59
3	16.33	7.2	18.92	17.93	44.51
4	16.37	8.5	16.73	16.54	47.96

PSA No. 7					
meas	N_u [N/V]	L_h [μm]	$s_{4,s}$ [μm] meas	$s_{4,s}$ [μm] sim	Cost [μVs]
1	16.43	0.8	24.41	24.23	49.17
2	16.40	3.2	21.55	21.80	48.34
3	16.36	7.0	19.15	18.06	42.42
4	16.32	8.4	16.56	16.66	45.82

PSA No. 8					
meas	N_u [N/V]	L_h [μm]	$s_{4,s}$ [μm] meas	$s_{4,s}$ [μm] sim	Cost [μVs]
1	16.39	1.0	24.28	24.10	50.16
2	16.35	3.4	21.63	21.67	49.74
3	16.33	6.8	18.92	18.28	45.34
4	16.37	8.0	16.73	17.02	48.24

PSA No. 9					
meas	N_u [N/V]	L_h [μm]	$s_{4,s}$ [μm] meas	$s_{4,s}$ [μm] sim	Cost [μVs]
1	16.33	0.8	24.66	24.21	55.80
2	16.28	3.3	21.98	21.82	51.45
3	16.26	7.0	19.27	18.18	48.89
4	16.29	8.5	17.18	16.68	49.08

PSA No. 10					
meas	N_u [N/V]	L_h [μm]	$s_{4,s}$ [μm] meas	$s_{4,s}$ [μm] sim	Cost [μVs]
1	16.46	0.4	24.83	24.64	50.40
2	16.44	3.2	21.65	21.68	46.17
3	16.42	6.0	19.38	18.89	43.08
4	16.45	8.4	16.77	16.67	44.59

6. Conclusions and outlook

This paper is concerned with the mathematical modelling and identification of a piezoelectrically driven control valve as it is used in direct fuel injection systems. The control valve constitutes a hybrid mechanical system consisting of a piezoelectric stack actuator (PSA) and the valve mechanics. It is well known that in large signal operation the PSA exhibits a nonlinear behaviour comprising hysteresis and creep effects. Furthermore, the constitutive parameters of piezoelectricity are subject to large variations according to changes in the temperature. In the literature, there exist a number of works which succeed in providing accurate models of the PSA over the whole operating range of interest. However, most of these models require too many signals to be measured or contain too many parameters to be adjusted to serve as an appropriate basis for the design of an online adaptation procedure. Other models require specific input signals for temperature adaptation.

Therefore, in this paper we derived a mathematical model for the PSA, which relies on the material model proposed by Goldfarb et al. [3] and solely contains one adaptation parameter. This parameter is a coupling coefficient between the mechanical and electrical variables and can be utilized to adjust the mathematical model to temperature changes and parameter variations in the series production. The price we have to pay for the simplicity of the model is that it only shows high accuracy for the charging phase of the PSA using typical input signals of the fuel injection process. The PSA model is combined with the mathematical model of the

Post-print version of the article: T. Müller, A. Kugi, G. Bachmaier, and M. Gerlich, "Modelling and identification of a piezoelectrically driven fuel injection control valve", *Mathematical and Computer Modelling of Dynamical Systems*, vol. 16, pp. 285–305, 2010. DOI: 10.1080/13873954.2010.502027

valve mechanics. Between the PSA and the valve piston there is small gap in the range of a few micrometers, also known as the idle stroke. The exact adjustment of the idle stroke value during the production process is quite difficult and time-consuming and the idle stroke value is also changing during operation, e.g. due to aging. This is why, apart from the coupling coefficient also the idle stroke value has to be identified. In this context, a crucial point is the modelling of the contact mechanics between the PSA and the valve piston. Due to the fast dynamics and the small sampling time of $0.5\,\mu$s, standard collision models from mechanics do not prove to be appropriate. Thus, a semi-empirical approach was pursued motivated by a number of experimental investigations.

The identification of the coupling parameter and the idle stroke value is based on the solution of a nonlinear parameter optimization problem. The idle stroke value could be successfully identified for four different values at room temperature and at 100°C as well as for ten different PSAs showing the robustness of the proposed approach against variations in the series production. The accuracy of the identified idle stroke values is in the range of $1\,\mu$m.

Up to now, the preload force was assumed to be constant. Thus, future research activities will have to address on the one hand the problem of varying load forces and on the other hand the reduction of the overall computational costs in view of a real-time implementation.

References

[1] C. Bartsch, *Piezo-Diesel-Direkteinspritzung: Historische Entwicklung und Stand der Technik bei Common-Rail und Pumpedüse*, Verlag Moderne Industrie, München, 2006.

[2] T. Hegewald, B. Kaltenbacher, M. Kaltenbacher, and R. Lerch, *Efficient Modeling of Ferroelectric Behavior for the Analysis of Piezoceramic Actuators*, in *Journal of Intelligent Material Systems and Structures*, vol. 19, no. 10, pp. 1117–1129, 2008.

[3] G. Goldfarb and N. Celanovic, *Modeling Piezoelectric Stack Actuators for Control of Micromanipulation*, in *IEEE Control Systems Magazine*, vol. 17, pp. 68–79, 1997.

[4] H. Adriaens, W. de Koning, and R. Banning, *Modeling Piezoelectric Actuators*, in *IEEE/ASME Transactions on Mechatronics*, vol. 5, pp. 331–341, 2000.

[5] K. Kuhnen, *Kompensation komplexer gedächtnisbehafteter Nichtlinearitäten in Systemen mit aktiven Materialien: Grundlagen - Erweiterte Methoden - Anwendungen*, Shaker, Aachen, 2008.

[6] S. Bashash and N. Jalili, *A Polynomial-Based Linear Mapping Strategy for Feedforward Compensation of Hysteresis in Piezoelectric Actuators*, in *Journal of Dynamic Systems, Measurement, and Control*, vol. 130, no. 3, pp. 031008.1–10, 2008.

[7] Q. Wang, *Piezoaktoren für Anwendungen im Kraftfahrzeug, Messtechnik und Modellierung*, Ph.D. diss., Ruhr-Universität Bochum, Bochum, 2006.

[8] C. Raupach, *Verfahren zur Stabilisierung der Kraftstoffdosierung bei Piezo-Einspritzventilen*, Ph.D. diss., Ruhr-Universität Bochum, Bochum, 2007.

[9] D. Mehlfeldt, H. Weckenmann, and G. Stöhr, *Modeling of piezoelectrically actuated fuel injectors*, in *Mechatronics*, vol. 18, no. 5–6, pp. 264-272, 2008.

[10] I.S. Committee, *IEEE Standard on Piezoelectricity (ANSI/IEEE Std 176-1987)*, IEEE, 1987.

[11] T. Ikeda, *Fundamentals of Piezoelectricity*, Oxford University Press, New York, 1990.

[12] W. Nowacki, *Dynamic Problems of Thermoelasticity*, Noordhoff International Publishing, PWN-Polish Scientific Publishers, Warszawa, 1975.

[13] H. Janocha, *Actuators: Basics and Applications*, Springer, Berlin, 2004.

[14] A. Visintin, *Differential Models of Hysteresis*, Springer, Berlin, Heidelberg, New York, 1994.

[15] P.R. Dahl and R. Wilder, *Math model of hysteresis in piezo-electric actuators for precision pointing systems*, in *Guidance and Control volumes of the Advances in the Astronautical Sciences*, vol. 57, pp. 61–88, 1985.

[16] F.J. Doyle and R.K. Pearson, *Identification and Control Using Volterra Models*, Springer, London, 2002.

[17] A. Kugi, D. Thull, and K. Kuhnen, *An infinite-dimensional control concept for piezoelectric structures with complex hysteresis*, in *Structural Control and Health Monitoring*, vol. 13, no. 6, pp. 1099–1119, 2006.

[18] O. Nelles, *Nonlinear System Identification*, Springer, Berlin, Heidelberg, 2001.

[19] W.J. Stronge, *Impact mechanics*, Cambridge Univ. Press, Cambridge, 2000.

[20] J.I. Imura and A.J. van der Schaft, *Characterization of Well-Posedness of Piecewise-Linear Systems*, in *IEEE Transactions on Automatic Control*, vol. 45, no. 9, pp. 1600–1619, 2000.

[21] J. van der Schaft and A.J. Schumacher, *An Introduction to Hybrid Dynamical Systems*, Springer, London, 2000.

Post-print version of the article: T. Müller, A. Kugi, G. Bachmaier, and M. Gerlich, "Modelling and identification of a piezoelectrically driven fuel injection control valve", *Mathematical and Computer Modelling of Dynamical Systems*, vol. 16, pp. 285–305, 2010. DOI: 10.1080/13873954.2010.502027